Bioorganic & Medicinal Chemistry Letters 21 (2011) 5684–5687

Contents lists available at SciVerse ScienceDirect

Bioorganic & Medicinal Chemistry Letters

journal homepage: www.elsevier.com/locate/bmcl

Discovery of PF-184563, a potent and selective V1a antagonist for the treatment of dysmenorrhoea. The influence of compound flexibility on microsomal stability

Patrick S. Johnson [a], Thomas Ryckmans [a,*], Justin Bryans [a], Dave M. Beal [a], Kevin N. Dack [a], Neil Feeder [b], Anthony Harrison [c], Mark Lewis [c], Helen J. Mason [a], James Mills [a], Julie Newman [a], Christelle Pasquinet [a], Dave J. Rawson [a], Lee R. Roberts [a], Rachel Russell [d], Deborah Spark [d], Alan Stobie [a], Toby J. Underwood [a], Robin Ward [d], Simon Wheeler [a]

[a] Pfizer Worldwide Medicinal Chemistry, Ramsgate Road, Sandwich Kent CT139NJ, UK
[b] Pfizer Pharmaceutical Development, Ramsgate Road, Sandwich Kent CT139NJ, UK
[c] Pfizer Department of Pharmacokinetics, Distribution and Metabolism, Ramsgate Road, Sandwich Kent CT139NJ, UK
[d] Pfizer Discovery Biology Ramsgate Road, Sandwich Kent CT139NJ, UK

ARTICLE INFO

Article history:
Received 11 July 2011
Accepted 6 August 2011
Available online 12 August 2011

Keywords:
V1a antagonists
Triazoles
LiPE
Lead optimisation
Number of rotatable bonds

ABSTRACT

The V1a receptor has emerged as an attractive target for a range of indications including Raynaud's disease and dysmenorrhoea. As part of an effort to discover a new class of orally active V1a antagonist, we optimised a highly lipophilic, metabolically unstable lead into a range of potent, selective and metabolically stable V1a antagonists. In this communication, we demonstrate the series-dependent effect of limiting the number of rotatable bonds in order to decrease Cytochrome P450-mediated metabolism. This effort culminated in the discovery of PF-184563, a novel, selective V1a antagonist with excellent in vitro and in vivo properties.

Vasopressin (AVP) is a small peptide that exerts its effects through the V1a, V1b, V2 and Oxytocin (OT) receptors.[1,2] The V1a receptor is expressed inter alia in smooth muscles, and its overactivation by elevated levels of AVP has been linked to both Raynaud's disease[3] and dysmenorrhoea. Clinical evidence shows that blockade of the V1a receptor by Relcovaptan **1** alleviates the symptoms of both these conditions.[3,4] As part of an effort to discover a new agent for the treatment of dysmenorrhoea, the triazole **2** attracted our interest as a novel V1a antagonist. An analog of this compound had been disclosed as a V1a antagonist.[5] (Fig. 1).

Despite modest potency and very high lipophilicity, compound **2** displayed a relatively high Ligand Efficiency[6] (LE) owing to its low molecular weight. Furthermore this chemotype is synthetically enabled, for example, each substituent on the triazole core can be introduced from widely available monomers (carboxylic acids and amines) using well-established methods. Early optimisation efforts on this lead focused on reducing the lipophilicity of the series, as high lipophilicity has been linked to a range of issues in development candidates, such as low solubility, high metabolic clearance, promiscuity and overall toxicity.[6,7]

The first key modification in this series was the replacement of the biaryl moiety of **2** with a 2-piperidyl pyridine group, resulting in compound **3**. Pleasingly, this compound proved to be only slightly less potent than **2** with a similar LE, and a *c*Log*P* reduced by 3 units. This translated into a much higher LiPE (4.4), a measure of binding efficiency per unit of lipophilicity and of overall lead quality.[8] Using this optimised 2-piperidyl pyridine scaffold, derivatives were prepared to further explore the SAR of the substituents at the 3- and 5-positions of the triazole.

Chemistry: The synthesis of compound **3** (R_1 = H) exemplifies the route to our final compounds **7a–f** and **8a–j**. Formation of bis-hydrazide **5** from the acid **4** was followed by a dehydrative cyclisation to oxadiazole **6**. Reaction of this oxadiazole with aniline formed the final triazole **3** in good yields. The full experimental details for the preparation of these compounds have been disclosed.[9,10] (Scheme 1).

Compounds **8a–d** were similarly obtained from the corresponding benzylamines; compound **8e** was prepared using butyryl hydrazide in step (a), while compounds **8f–j** were prepared by nucleophilic substitution from the corresponding 5-chloromethyl

* Corresponding author. Tel.: +44 1304 643 735; fax: +44 1304 651 817.
E-mail address: Thomas.ryckmans@gmail.com (T. Ryckmans).

0960-894X/$ - see front matter © 2011 Elsevier Ltd. All rights reserved.
doi:10.1016/j.bmcl.2011.08.038

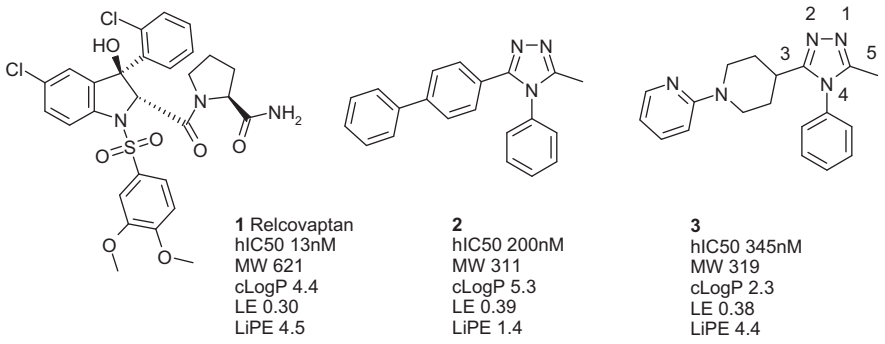

Figure 1. Structure of Relcovaptan **1** and lead **2**.

oxadiazole **9** (see Scheme 2) followed by step (c) using benzylamine.[9–11]

Results and discussion: Selected examples are presented here. For *N*-phenyl derivatives **7**, substituents such as 4-methoxy (**7a**), 4-methyl (**7c**) and 4-chloro (**7f**) proved beneficial to potency at the V1a receptor, with a concomitant increases in LiPE. The 4-CN and 4-CF_3 groups were poorly tolerated. Disappointingly, our most potent compound **7f** suffered from significant metabolic instability as measured in Human Liver Microsomes (HLM). Next, a series of *N*-benzyl derivatives was prepared. In this case, the 3-chloro compound (**8c**) displayed interesting potency but with similar metabolic liability to **7f**. Modification of the side chain at the 5-position of the triazole demonstrated that while basic (**8h**) and acidic (**8i**) groups were poorly tolerated, both lipophilic and polar side chains were beneficial to potency (compare **8a** with **8e** and **8f**). The best LiPE value was achieved with compound **8j**. Combination of the features of **8c** (R_1 = 3-Cl) and **8c** (R_2 = 2*H*-[1,2,3]triazolyl–) in **8k** proved to be additive in terms of potency, but also resulted in high metabolic instability. All potent derivatives **8** proved metabolically unstable despite their low *c*Log*P* values (Table 1).

In order to define a strategy to reduce microsomal clearance, we sought to find a correlation between HLM clearance and physicochemical properties using a larger dataset (60 compounds). Attempts to correlate *c*Log*P* with HLM clearance (a well established trend) were not successful, possibly because of the limited range of lipophilicity exemplified (85% of prepared compounds had *c*Log*P* values between 1 and 3). Another molecular descriptor linked to microsomal clearance is the number of rotatable bonds (NRB); compounds with high NRB (high flexibility) are more likely to adopt a conformation recognised by Cytochrome P_{450}. Indeed, plotting HLM clearance binned between low ($Cl_{int} < 10$), medium ($10 \leqslant Cl_{int} \leqslant 20$) and high ($Cl_{int} > 20$) values against NRB values showed that all stable compounds bar one (with a low *c*Log*P* of 0.6) had a NRB count below 5. Conversely, all compounds with a NRB > 7 displayed a high clearance, even at low *c*Log*P* values. (Fig. 2)

This analysis, albeit based on a limited dataset, led us to design a series of compounds in which conformational restriction was achieved by tethering the 3- and 5-substituents of the triazole. Reaction of chloromethyl oxadiazole **9** with bis nucleophiles **10** afforded the adduct **11**, which was cyclised under acidic conditions to give tethered compounds **12** and **13**. Full experimental details for the preparation of these compounds have been disclosed.[11–13] Cyclic ethers **12** proved mostly equipotent to their non-cyclic analogs, but generally displayed a trend toward higher metabolic stability (compare **12a** and **3**, **12c** and **7a**, **12d** and **7f**). This trend can be attributed to either (or both) the reduction in *c*Log*P* or NRB count for compounds **12a–d** compared with compounds **3** and

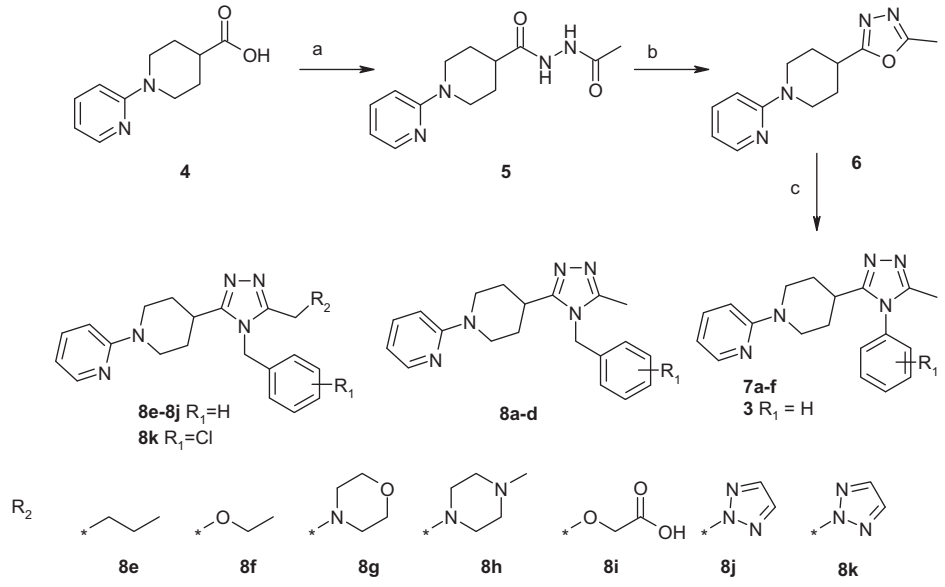

Scheme 1. Typical procedure for the synthesis of compound **6**. Reagents and conditions (a) oxalyl chloride (2 equiv), DCM, 25 °C, 16 h then acetylhydrazide (2 equiv), DCM, 25 °C, 16 h, 39%; (b) $POCl_3$ (excess), 100 °C 2 h 95%; (c) aniline or benzylamine (4 equiv), anhydrous $MgCl_2$ (0.3 equiv), 150 °C 18 h 75%, or xylene, *p*TSA (0.01 equiv), reflux 18 h.

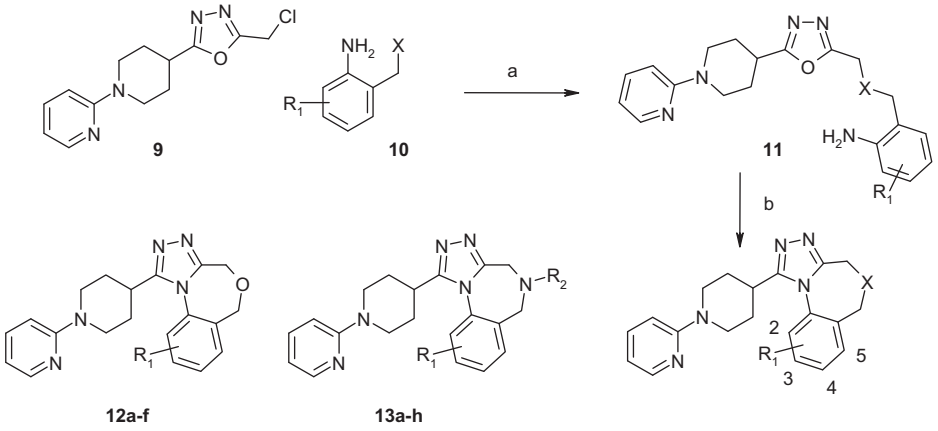

Scheme 2. Typical procedure for the synthesis of compounds **12** and **13**. Reagents and conditions (a) X = OH: NaH, THF, 25 °C, 3 h, 72%, X = NH_2, THF, 50°C, 18 h, 75%; (b) xylene, *p*TSA (0.01 equiv), reflux 18 h, X = OH: 65%, X = NH:76%.

Table 1
Antagonist activity[a] at the human V1a receptor

Compound	R_1	hV1a IC_{50} (nM)	*cLogP*	LiPE	HLM Cl_{int}[b]
2	—	200	5.3	1.4	n/a
3	H	345	2.3	4.4	<8
7a	4-OMe	133	2.4	4.8	11
7b	2-Me	199	2.8	4.2	33
7c	4-Me	71	2.8	4.6	40
7d	4-CN	2310	1.8	4.2	<8
7e	4-CF_3	580	3.2	3.3	n/a
7f	4-Cl	9	3.1	5.3	23
8a	H	117	1.8	5.4	<8
8b	3-Me	83	2.3	5.1	23
8c	3-Cl	29	2.5	5.4	29
8d	4-Me	1450	2.3	3.9	19
8e	H	17	3.4	4.7	154
8f	H	20	1.7	6.3	23
8g	H	25	1.3	6.7	34
8h	H	609	1.8	4.7	n/a
8i	H	2460	0.8	5.1	<8
8j	H	18	1.1	7.0	19
8k	Cl	3	1.8	6.9	104

[a] Values are geometric means of a minimum of two experiments.
[b] In vitro Human Liver Microsomal Intrinsic Clearance, expressed in μL/min/mg.

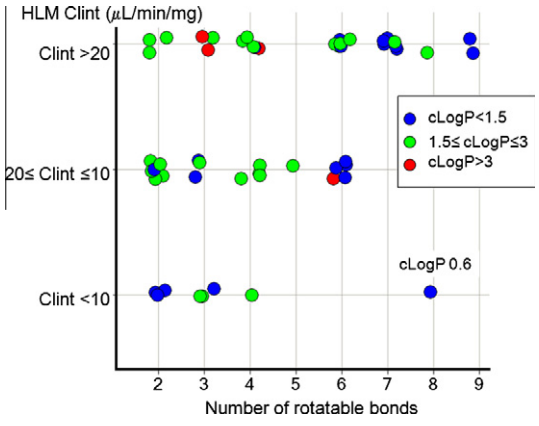

Figure 2. Relationship between NRB and HLM Cl_{int}. Individual points have been jittered to avoid superposition. Legend: Blue: *cLogP* < 1.5, Green, *cLogP* between 1.5 and 3, Red: *cLogP*>3.

7a–f. 4-substitution was beneficial to potency, but chlorine atoms in the 3- or 5-positions were poorly tolerated (**12d** vs **12d** and **12f**) (Scheme 2).

Table 2
Antagonist activity[a] of cyclic derivatives **12** and **13** at the human V1a receptor

Compound	R_1	R_2	hV1a IC_{50} (nM)	*cLogP*	LiPE	HLM Cl_{int}[b]
12a	—	—	345	1.0	5.8	<8
12b	4-Me	—	20	1.5	6.5	11
12c	4-OMe	—	135	1.0	6.1	<8
12d	4-Cl	—	17	1.7	6.4	15
12e	3-Cl	—	5380	1.7	3.9	<8
12f	5-Cl	—	904	1.7	4.7	32
13a	—	H	4480	1.0	4.7	n/a
13b	Cl	H	110	1.7	5.6	n/a
13c	—	Me	272	1.4	5.5	n/a
13d	Cl	Me	6.7	2.1	6.3	14
13e	Cl	CO_2Me	3.2	2.7	6.1	n/a
13f	Cl	SO_2NMe_2	0.5	1.3	8.3	182
13g	Cl	COMe	4.8	0.7	7.9	9
13h	Cl	SO_2Me	1.3	2.5	6.7	n/a

[a] Values are geometric means of a minimum of two experiments.
[b] In vitro Human Liver Microsomal Intrinsic Clearance, expressed in μL/min/mg.

These results prompted us to prepare cyclic amines **13**. Unsubstituted derivative **13a** was surprisingly weak at the V1a receptor, but addition of a 4-Chloro substituent improved potency 40-fold (**13b**). N-Methylation (**13c**) also increased potency 16-fold. Gratifyingly, the combination of these features in **13d** proved additive, with a 670-fold increase of potency ($16 \times 40 = 640$) between **13a** and **13d**. This compound also displayed adequate metabolic stability. Further N-substituted derivatives **13e–h** were prepared, resulting in a range of very potent compounds (Table 2).

The single crystal X-ray structures of **13d** and **13g** were solved, the two structures differing mainly in torsion angles across the two rotatable bonds[14] (Fig. 3).

Compounds **13d**, **13e**, **13g**, and **13h** were further evaluated in a panel of in vitro assays. No significant inhibition of Cytochrome P_{450} (IC_{50} values >30 μM for CYP 1A2, 2C9, 2C19, 2D6 and 3A4) or blockade of the hERG channel[15] were observed. The compounds showed little binding to V1b or OT receptors (>10 μM) (Table 3).

While compounds **13d**, **13g**, and **13h** displayed weak binding to the hV2 receptor, **13e** and **13h** proved to be potent agonists of this receptor and not progressed further. The 40-fold V2-V1a selectivity window for **13d** and **13g**, while not optimal, was deemed acceptable at the time. Good cell permeability was predicted for both **13d** and **13g** using the Caco-2 model (Papp A/B and B/A of 29/28 and 17/27 10^{-6} cm/sec respectively). Compounds **13d** and **13g** were profiled over 70 targets (Cerep Panel), producing less than 30% inhibition of binding at 10 μM on all targets. Finally, both

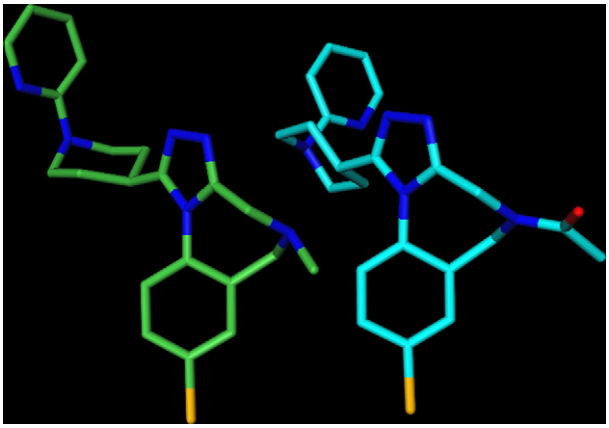

Figure 3. Single crystal X-ray structures of **13d** (green) and **13g** (cyan).

Table 3
Activity of cyclic derivatives **13** at the hV1a receptor, the hV2 receptor (in agonist and antagonist modes) and the hERG channel

Compound	hV1a IC_{50}[a] (nM)	hV2 EC_{50}[a] (nM)	hV2 IC_{50}[a] (nM)	hERG IC_{50}[b] (nM)
13d	6.7	265	8490	17,900
13e	3.2	31	n/a	47,300
13g	4.8	215	4500	35,200
13h	1.3	13	715	30,700

[a] Values are geometric means of a minimum of two experiments.
[b] Values are obtained from a single experiment.

Table 4
In vivo PK parameters of PF-184536 (**13d**) following iv and po administration of 2 mg/kg ($n = 2$, Sprague–Dawley rats) and single-specie scaling predictions for human PK parameters

Parameter	Measured values (rat)	Predicted values (human)
T_{max} (h)	0.8	–
C_{max} (ng/mL)	97	–
F (%)	34	75%
Cl (mL/min/kg)	51	6.4
V_d (L/kg)	2.7	2.0
$t_{1/2}$ (h)	1.8	3.5
Ppb (% bound)	69%	77%[a]

[a] Measured human plasma protein binding value.

compounds were evaluated in the Ames[16] and the CHO in vitro micronucleus assays. While compound **13g** was positive in the micronucleus assay, **13d** (PF-184536) did not induce microbial gene mutations or chromosomal abnormalities in vitro. The pharmacokinetic properties of this compound were measured in the rat (2 mg/kg), demonstrating the favorable profile of PF-184536. There was no significant biliary or renal clearance of PF-184563 in bile duct cannulated rats. The major metabolic route in rat was N-demethylation to **13b**. The main metabolite of PF-184536 by human hepatocytes and microsomes was the inactive pyridine N-oxide, but minor N-demethylation was also observed. Human PK estimations using single-specie scaling[17] based on rat PK data predicted good absorption ($F = 75\%$) and half-life of 3.5 h,[18] suitable for oral administration using controlled release (Table 4).

In conclusion, we have reported the discovery of PF-184563, a potent, selective V1a antagonist suitable for human studies. Modifications of a highly lipophilic substrate allowed us to identify a new class of polar V1a antagonists. A relationship between molecular flexibility (as measured by the number of rotatable bonds) and in vitro metabolic stability was identified, resulting in the design of a class of rigid, tethered compounds **13**. This effort culminated in the discovery of PF-184563 (**13d**), a potent, selective V1a antagonist suitable for human clinical studies. The full pharmacological profile of PF-184563 will be presented separately.

Supplementary data

Supplementary data associated with this article can be found, in the online version, at doi:10.1016/j.bmcl.2011.08.038.

References and notes

1. Ryckmans, T. *Curr. Opin. Drug Disc. Dev.* **2010**, *13*, 538.
2. Ryckmans, T. *Annu. Rep. Med. Chem.* **2009**, *44*, 129.
3. Hayoz, D.; Bizzini, G.; Noël, B.; Depairon, M.; Burnier, M.; Fauveau, C.; Rouillon, A.; Brouard, R.; Brunner, H. R. *Rheumatology* **2000**, *39*, 1132.
4. Brouard, R.; Bossmar, T.; Fournié-Lloret, D.; Chassard, D.; Åkerlund, M. *BJOG: Int. J. Obstetrics Gynaecol.* **2000**, *107*, 614.
5. Kakefuda, A.; Suzuki, T.; Tobe, T.; Tsukada, J.; Tahara, A.; Sakamoto, S.; Tsukamoto, S. *J. Med. Chem.* **2002**, *45*, 2589.
6. Leeson, P. D.; Springthorpe, B. *Nat. Rev. Drug Disc.* **2007**, *6*, 881.
7. Hughes, J. D.; Blagg, J.; Price, D. A.; Bailey, S.; DeCrescenzo, G. A.; Devraj, R. V.; Ellsworth, E.; Fobian, Y. M.; Gibbs, M. E.; Gilles, R. W.; Greene, N.; Huang, E.; Krieger-Burke, T.; Loesel, J.; Wager, T.; Whiteley, L.; Zhang, Y. *Bioorg. Med. Chem. Lett.* **2008**, *18*, 4872.
8. Ryckmans, T.; Edwards, M. P.; Horne, V. A.; Correia, A. M.; Owen, D. R.; Thompson, L. R.; Tran, I.; Tutt, M. F.; Young, T. *Bioorg. Med. Chem. Lett.* **2009**, *19*, 4406.
9. Armour, R. D.; Baxter, A. D.; Bryans, J. S.; Dack, K. N.; Johnson, P. S.; Lewthwaite, R. A.; Newman, J.; Rawson, D. J.; Ryckmans, T. Application: WO 2004037809; **2004**.
10. Bryans, J. S.; Johnson, P. S.; Ryckmans, T.; Stobie, A. WO 92,005,079,808, 2005.
11. Ellis, D.; Johnson, P. S.; Nortcliffe, A.; Wheeler, S. *Synth. Commun.* **2010**, *40*, 3021.
12. Beal, D. M.; Bryans, J. S.; Johnson, P. S.; Newman, J.; Pasquinet, C.; Peakman, T. M.; Ryckmans, T.; Underwood, T. J.; Wheeler, S. Submitted to *Tetrahedron Lett.* **2011**.
13. Bryans, J. S.; Johnson, P. S.; Ryckmans, T.; Stobie, A. WO2004074291, 2004.
14. The following crystal structures have been deposited at the Cambridge Crystallographic Data Centre and allocated the deposition numbers CCDC 836796 & 836797.
15. Singleton, D. H.; Boyd, H.; Steidl-Nichols, J. V.; Deacon, M.; de Groot, M. J.; Price, D.; Nettleton, D. O.; Wallace, N. K.; Troutman, M. D.; Williams, C.; Boyd, J. G. *J. Med. Chem.* **2007**, *50*, 2931.
16. Aubrecht, J.; Ku, W. W.-T.; Osowski, J. J. Application: EP 1217077; **2002**.
17. Hosea, N. A.; Collard, W. T.; Cole, S.; Maurer, T. S.; Fang, R. X.; Jones, H.; Kakar, S. M.; Nakai, Y.; Smith, B. J.; Webster, R.; Beaumont, K. *J. Clin. Pharmacol.* **2009**, *49*, 513.
18. Single-specie scaling of rat unbound clearance was carried out using correlations of human/rat unbound clearance values for 44 drugs using the following equation:

$$\text{Log}\ (\text{Cl}_u\ \text{human}) = 0.9285 \times \text{Log}(\text{Cl}_u\ \text{rat}) - 0.6171 (r^2 = 0.89)$$

The human unbound volume is assumed to be the same as the animal species in which the pharmacokinetics were measured.